

BROADBAND LUMINESCENCE IN NANOSTRUCTURED GLASSES

N. V. Golubev,^{1,3} E. S. Ignat'eva,¹ R. Lorenzi,² A. Paleari,^{1,2} V. N. Sigaev^{1,4}

Translated from *Steklo i Keramika*, No. 4, pp. 14 – 20, April, 2013.

The mechanism of broadband near-IR luminescence in the process of nanostructuring of Ni^{2+} -activated glasses in the system $\text{R}_2\text{O}-\text{Ga}_2\text{O}_3-\text{SiO}_2-\text{GeO}_2$ ($\text{R} = \text{Li}, \text{Na}$) at the initial stage of phase separation is described.

Key words: broadband luminescence, Ni^{2+} , low-angle neutron scattering, nanouniformity, $\gamma\text{-}\text{Ga}_2\text{O}_3$.

An important alternative to crystals as matrices for doping with ions of *d*-elements could be glasses, whose advantages are relatively low cost, possibility of obtaining articles of practically any size and shape, including in the form of fiber, possibility of changing the properties purposefully by varying the composition and so on. However, because the probability of nonradiative transitions is high in glasses the luminescence of transition element ions is largely suppressed. One approach to solving this problem is to form in the interior of the glass phase nonuniformities of a crystalline nature, combining active properties of the crystalline phase and the advantages of the glassy matrix in a single material.

Optical nonlinearity can be initiated in glass as a result of structural transformations at the initial stages of phase separation [1] and the spectral-luminescence properties can be improved as a result of the coloring impurity entering the structure of the precipitated crystalline phase [2]. The optical properties of the material can be controlled by changing the volume fraction, size and structure of the crystals in the glass, which opens up new possibilities for developing laser and luminescent media.

One of the main drawbacks of such materials is light scattering by the interphase boundary. It can be minimized by decreasing the difference Δn between the refractive indices of the glass phase and the crystals and/or the precipitation of very small particles — 2 – 10 nm in size [3], much smaller than the typical sizes of crystallites in classical sitals, whose appearance and development in Russia is associated, first and foremost, with the scientific school of I. I. Kitaigorodskii.

In recent years a large number of works have been associated with transparent glass ceramic materials based on oxide phases doped with ions of transition elements, specifically, Ni^{2+} [4 – 15]. Such glass ceramic materials are of interest because of the possibility of obtaining broadband near-IR luminescence in them and developing based on them radiation sources for optical coherent tomography, fiber amplifiers and tunable lasers used in fiber-optic communication lines, systems for remote sensing of the Earth and so on. In this respect the low-alkali gallium-silicon-germanate glasses, information about which is still limited [12 – 13], are of interest. The prospects for glass ceramic materials based on them, combining the required spectral-luminescence properties with the possibility of obtaining the initial glass at temperatures below 1500°C, makes it necessary to study the existing data in detail when comparing with close low-alkali gallium-silicate glasses.

LOW-ALKALI GALLIUM-SILICATE GLASSES

It is shown in a number works that a transparent glass ceramic based on spinel ZnAl_2O_4 [4], MgAl_2O_4 [5], $\gamma\text{-}\text{Ga}_2\text{O}_3$ [6], LiGa_5O_8 [7 – 10] and the phase $\beta\text{-}\text{Ga}_2\text{O}_3$ [11] can be obtained in silicate glasses, and broadband (about 250 – 340 nm) luminescence in the near-IR range as a result of Ni^{2+} entering nanocrystals which precipitated in the interior volume of the glass has been recorded. Of the indicated crystalline phases the gallate phases merit special attention. They possess a long luminescence decay constant and high quantum yield at room temperature [9, 11], and for this reason the glasses crystallizing with their precipitation will be examined in detail below. The wavelength corresponding to the maximum of the luminescence band (about 1200 – 1440 nm) and the lifetime of the luminescence (60 – 1100 μsec) vary strongly in the glass ceramic material listed. It is impossible to compare them according to these parameters because the

¹ P. D. Sarkisov International Laboratory of Glass-Based Functional Materials, D. I. Mendelev Russian Chemical Technology University, Moscow, Russia.

² University of Milan-Bikoka, Milan, Italy.

³ E-mail: golubev_muctr@mail.ru.

⁴ E-mail: vlad.sigaev@gmail.com.

heat-treatment conditions are not comparable. In addition, in the overwhelming majority of the cases there is no information on the correction to the luminescence spectrum taking account of the spectral sensitivity of the detector, which also hampers comparison. However, often, the strength of the crystal field determines the lifetime and band maximum of the luminescence [11] — as the field increases in strength the band maximum shifts in the direction of shorter wavelengths and the lifetime increases.

In [16] it was noted that the lifetime and the relative intensity of the luminescence increase sharply when Ga_2O_3 is introduced into glass crystallizing with spinel MgAl_2O_4 precipitating. The authors attribute this increase to an increase in the amount of a crystalline phase doped with Ni^{2+} , but mainly to a change in the cation distribution over the crystallographically nonequivalent positions in the spinel structure, resulting in an increase of the Ni^{2+} fraction in an octahedral environment. It is known that if several different cations are present in the crystal, then it is possible for nonequivalent positions to be occupied differently. The general formula of spinel group crystals is $AB_2\text{O}_4$ (A — divalent, B — trivalent metal) and such crystals belong to the cubic system. In the so-called normal spinels, which MgAl_2O_4 is, the A cations occupy tetrahedral positions and the B cations are found in the octahedral sites. The energy of preference for a definite coordination number in this structure, which is the difference between the energies of stabilization of cations in nonequivalent positions of the crystal structure, plays an important role in the explanation of the cation distribution [17]. The energy of preference to A positions in the spinel lattice is higher for Ga^{3+} than for Ni^{2+} [18], so that as the number of Ga^{3+} ions in the MgAl_2O_4 structure increases more and more Ni^{2+} ions occupy octahedral positions, whose symmetry gives rise to the near-IR luminescence of Ni^{2+} . In addition, the increase of the lifetime of the luminescence when Al^{3+} is replaced by the heavier Ga^{3+} is determined by the lower probability of non-radiative processes as a result of a decrease of the frequencies of the main vibrational transitions [19].

In summary, the transparent crystalline materials containing oxide gallate phases, luminescing on doping with transition-element ions in the near-IR region, are of special interest. In addition, these phases can also luminesce in the visible range on excitation with UV radiation [20], which gives rise to the possibility of using materials based on them for UV radiation detection and visualization (solar-blind detectors). The spectral-luminescence characteristics of low-alkali gallium-silicon-germanate glasses in the visible range are being actively studied in our laboratory. It is also worth noting that alkali gallium-silicate glasses are much easier to obtain and are less prone toward crystallization than the analogous aluminum-silicate glasses [21].

The luminescence of the glass ceramic materials based on β -, γ - Ga_2O_3 or LiGa_5O_8 nanocrystals doped with Ni^{2+} ions has been repeatedly observed in the gallium-silicate system with low alkali content [6, 7 – 10, 11]. The data on this

system are incomplete and limited mainly to information on the presence of near-IR luminescence, bandwidths at half-height, lifetime and calculations of the crystal field parameters in heat-treated glasses based on the absorption data. In addition, a rough Scherrer estimate of the sizes of nanocrystals is available; in rare cases it is supplemented by the results of transmission electron microscopy [6, 9, 11]. Several works are devoted to measuring the intensity and determining the position and shape of the luminescence band at different temperatures [7], under different heat-treatment conditions [6] and with the introduction of a sensitizer [10]. Only one work devotes attention to crystallization of glasses in the system $\text{Li}_2\text{O}-\text{Ga}_2\text{O}_3-\text{SiO}_2-\text{NiO}$ but without any relation to the luminescence characteristics [8]. The mechanisms of the formation of nano-nonuniformities in these glasses as well as their effect on the optical characteristics have been still little studied. It should be noted that in the works indicated only laboratory samples of glasses were made at temperatures not lower than 1580°C and over several (at least 2) hours. This means a temperature increase accompanying a transition to large melting volumes with the required operations of swirling and mixing, making it difficult to obtain initial glass that is optically uniform. Glass melting in platinum crucibles at such high temperatures causes the crucible to break down rapidly and appreciable quantities of atomic platinum to enter the glass, which sharply reduces its radiation resistance [22].

The key problems are to determine the correlations between the nanostructure and optical properties, the need to decrease Δn by increasing the refractive index in the glassy matrix, the search for new compositions in order to lower the glassmaking temperature of low-alkali gallium-silicate glasses and obtaining them in the form of optical-quality glasses while preserving the possibility of purposefully changing their nano-nonuniform structure. The solutions open the way to practical applications of this new class of glass ceramic materials.

LOW-ALKALI GALLIUM-SILICON-GERMANATE GLASSES

In one of the first works on the properties and structure of the system $\text{R}_2\text{O}-\text{Ga}_2\text{O}_3-\text{GeO}_2$ ($\text{R} = \text{Li}, \text{Na}, \text{K}$) it is noted that the glass forming region is wider than in $\text{R}_2\text{O}-\text{Al}_2\text{O}_3-\text{GeO}_2$ [23], while the melting temperature is $1200 - 1450^\circ\text{C}$, depending on the composition. Heat treatment of similar gallate glasses results in undesirable crystallization of ancillary phases that can be suppressed by replacing some gallium oxide with silicon oxide [12]. The synthesis temperature of low-alkali gallium-silicon-germanate glasses does not exceed 1500°C , which is at least 80°C lower than for silicate systems. In the present work it is concluded that LiGa_5O_8 was exclusively precipitated in the interior volume in 0.1 NiO doped glass with the composition (mol. %) 7.5 Li_2O , 2.5 Na_2O , 20 Ga_2O_3 , 35 GeO_2 and 35 SiO_2 after heat-treat-

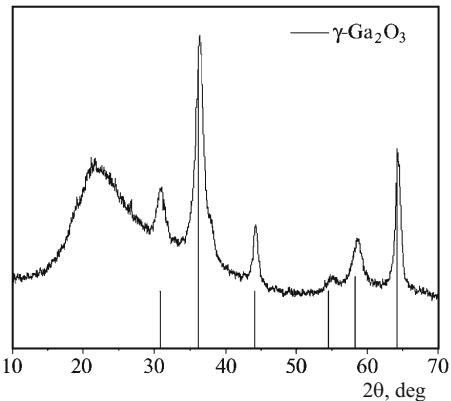


Fig. 1. X-ray diffraction pattern of Ge35-0.1 glass heat-treated at 690°C for 18 h and the line diffraction patterns of γ -Ga₂O₃ (card No. 20-0426 from the JCPDS electronic catalogue of diffraction patterns).

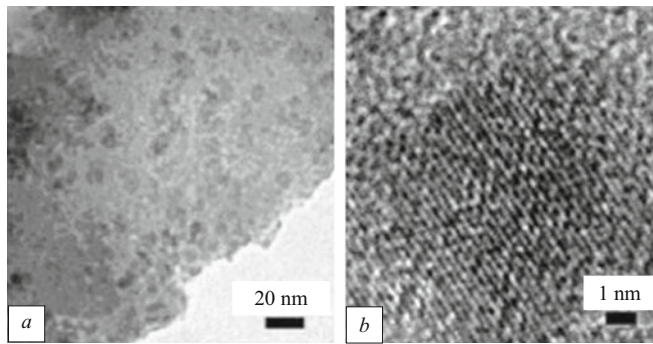


Fig. 2. Electronic photographs of heat-treated (690°C, 15 min) Ge35-0.1 glass.

ment. This composition is denoted as Ge35 with subsequent indication of the molar content NiO from 0.01 to 1%. The similarity of the line diffraction patterns of the phases LiGa₅O₈ and γ -Ga₂O₃ makes them difficult to distinguish, including in the diffraction patterns of heat-treated glasses. However, a comparison of the relation between the intensities of the Bragg reflections at 36.2° and 64.5° in the x-ray diffraction patterns of heat-treated glasses and the data in the card catalogues shows that the phase γ -Ga₂O₃, where some Ga³⁺ ions are replaced with Li⁺, precipitates predominately (Fig. 1). According to the x-ray diffraction patterns the precipitation mainly of γ -Ga₂O₃ in low-alkali gallium-silicate glasses is also present in works where it is concluded that only LiGa₅O₈ is present in heat-treated samples [7–9]. To gain a deeper understanding of the process controlling the phenomena accompanying phase separation of low-alkali gallium-silicate-germanate glasses it is necessary to study their crystallization in detail, including at the late stages of the process. We are currently engaged in making such an investigation. The few existing data, mainly from our recent works [13, 15], are examined below.

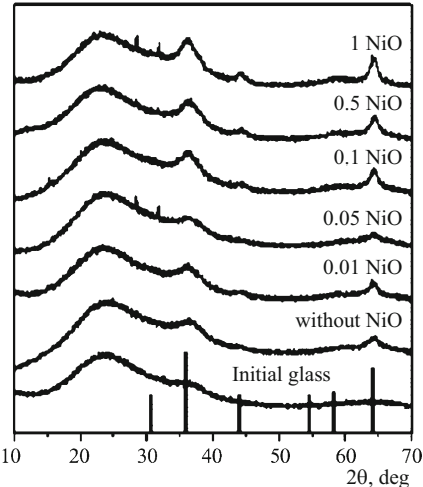


Fig. 3. X-ray diffraction patterns of plates of initial and heat-treated Ge35 glass with different NiO molar content.

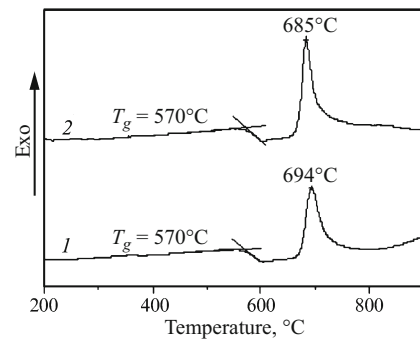


Fig. 4. DSC curves of monolithic samples of glass with the compositions Ge35 (1) and Ge35-0.1 (2).

Irrespective of the treatment duration at the temperature of the exothermal peak (about 690°C) in glasses with different NiO content, the size of the phase nonuniformities is about 6 nm according to the transmission electron microscopy (TEM) data (Fig. 2a), which in the main is close to the size in low-alkali gallium-silicate glasses (about 10 nm). In turn, high-resolution photographs have confirmed the crystalline nature of the precipitated nanoparticles with heat-treatment times 15 min and longer (Fig. 2b). As the NiO concentration increases, the intensities of the Bragg reflections of the high-gallate phase in the diffraction patterns of plates of heat-treated glasses increase, and at the same time the ratio of the integrated area of the diffraction peaks and amorphous halo in the experimental samples remains practically unchanged (Fig. 3). The shift of the temperature at the maximum of the exothermal peak toward low temperatures in comparing the DSC curves for glasses with and without NiO (Fig. 4) and a comparison of the TEM and XPA data show that the Ni²⁺ ions intensify the proneness of the glass toward crystallization without, however, significantly increasing the amount of the crystalline phase.

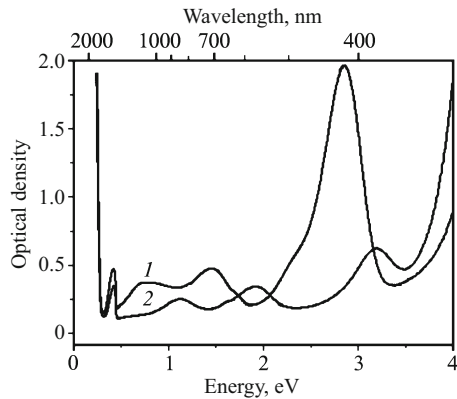


Fig. 5. Light attenuation spectrum of samples (thickness 2 mm): 1) initial; 2) heat-treated (690°C , 15 min) Ge35-1 glass.

Comparing the light attenuation spectra of the initial and heat-treated glasses with different NiO content showed that among the characteristic for heat-treated samples absorption bands at 390, 650 and 1100 nm, which correspond to electronic transitions of Ni^{2+} ions in an octahedral environment, there is no strongest absorption band near 435 nm, characteristic for Ni^{2+} ions in glass (Fig. 5). This signifies practically complete absence of Ni^{2+} ions in glass and, therefore, their transition into nanocrystals which precipitated in the interior volume of the glassy matrix. The strict linear relation between the integrated area of the Ni^{2+} absorption bands in heat-treated samples and the computed amount of NiO in the glasses (data not presented) also supports the idea that these ions predominately enter into the crystalline phase. It is worth noting that the investigated NiO concentration range is quite wide — from 3.6×10^{18} to $3.5 \times 10^{20} \text{ cm}^{-3}$.

The preference for Ni^{2+} ions to enter the structure of nanocrystals, whose symmetry ensures the required spectral properties of this ion, results in the appearance in heat-treated samples of near-IR broadband luminescence (Fig. 6). In addition, samples with 0.1 mol.% NiO exhibited the maximum luminescence intensity. The luminescence spectra obtained with excitation at 980 nm are similar to the spectra presented, but the quantum efficiency of the luminescence is higher (about 10% instead of 1%). The maximum of the luminescence band depends on the NiO content, shifting in the direction longer wavelengths with increasing NiO concentration (see Fig. 6).

In comparing different samples, the value of the effective lifetime of the luminescence varied from 360 μsec in the glass ceramic material with the lowest NiO molar content (0.01%) to 10 μsec in the sample with the maximum NiO content (1%). A sharp decrease of the luminescence lifetime was observed for NiO molar content 0.1%. The average distance between Ni^{2+} ions was calculated on the basis of the kinetics of luminescence decay. Depending on the NiO content it varied from 1 to 5 nm. Likewise, the critical inter-ion distance for resonance energy transfer (Förster radius) was found to be 1.4 nm.

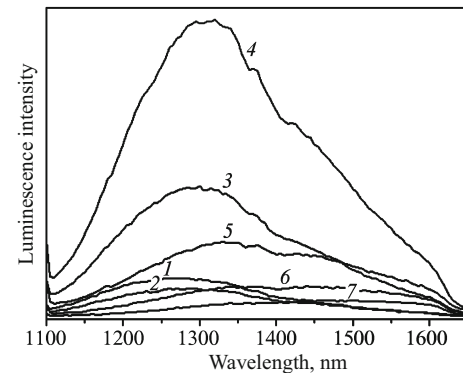


Fig. 6. Luminescence spectra ($\lambda_{\text{exc}} = 635 \text{ nm}$) of heat-treated (690°C , 15 min) Ge35 glasses with different NiO molar content (mol.%): 1) 0.01, 2) 0.05, 3) 0.07, 4) 0.1, 5) 0.3, 6) 0.5, 7) 1.

In [24], it is proposed on the basis of the x-ray diffraction patterns of the initial lithium-gallium-silicate glass, demonstrating a wide small shoulder near 30° , that phase nano-nonuniformities are present already in the hardened sample. However, low-angle neutron scattering (LANS) was not used in this or any subsequent work to perform studies at the initial stages of phase separation.

LANS has been used to study phase separation at pre-crystallization stages at temperatures where Ge35-0.1 glass was transparent after treatment. The presence of one maximum on the LANS curves of all samples indicates that there exists only one type of region of nonuniformity, i.e., close to a monodisperse size distribution of these regions. This conclusion agrees with the TEM results (see Fig. 2). The weakly expressed maximum in the LANS curve of the initial gallium-silicon-germanate glass likewise indicates the presence in hardened samples of phase nano-nonuniformities which cannot be found by means of TEM. The following scheme of structural transformations of the experimental glasses can be proposed on the basis of the LANS data.

The first process, leading to the appearance of nonuniformities in them, is phase separation of the liquid type, occurring as the melt cools. This is evidenced by the absence of Bragg reflections in the x-ray diffraction pattern of the initial glass and the presence of a weakly expressed maximum in the low-angle curve. The size of these initial nonuniformities, determined from the gyration radius R_g according to the slope of the Guinier section [25], is 8 nm. In the initial glass the average distance between the centers of the scattering regions is given approximately by $d = 2\pi/q_{\max}$, where q_{\max} corresponds to the maximum intensity of scattering and is about 20 nm. With heat-treatment (near T_g) of the hardened glass the regions of nonuniformities shrink to about 2 nm, which is accompanied by a shift of the maximum on the LANS curves toward larger values of the scattering vector (Fig. 7). This attests to a decrease of the distance between the centers of the scattering regions and indicates decay of the initial phase nano-nonuniformities and an increase of

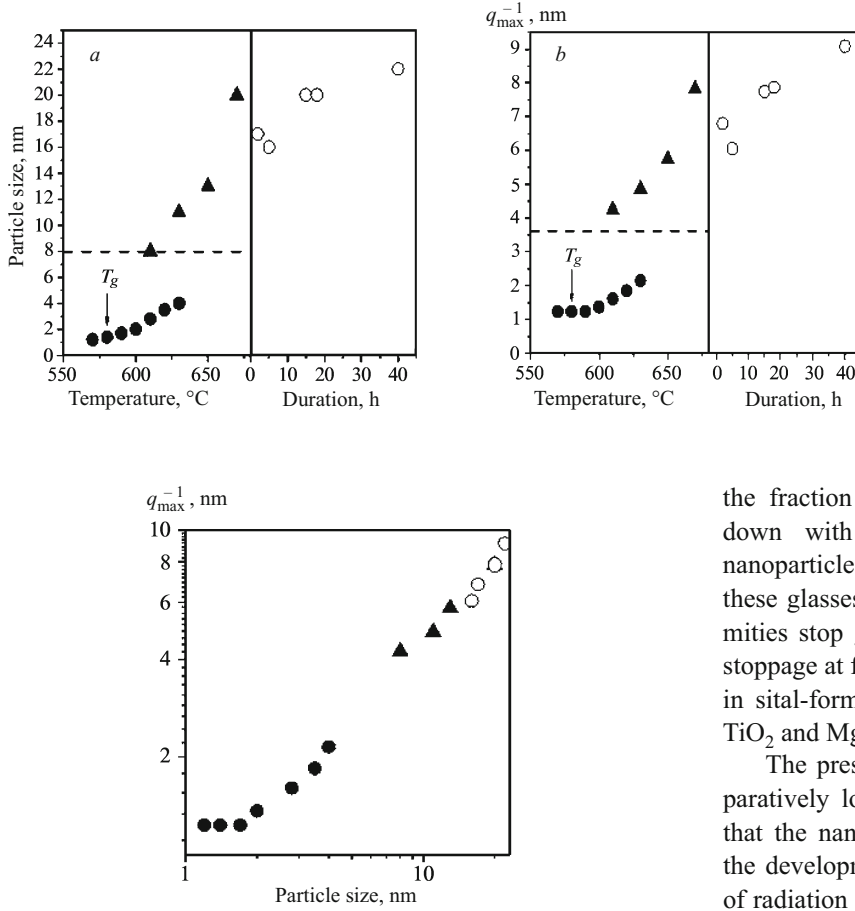


Fig. 8. q_{\max}^{-1} versus the size of the nonuniformities in logarithmic coordinates.

their total number, i.e., the occurrence of secondary liquation processes [25].

Subsequent heat-treatment (from $T_g = +30^\circ\text{C}$ to temperatures near the exothermal peak) increases the size of the nano-nonuniformities (from < 2 to 20 nm) and shifts the LANS maximum to lower values of the scattering vector. Figures 7 and 8 display the sizes of the nonuniformities and the reciprocal of the scattering vector at the maximum of the low-angle curve, q_{\max}^{-1} , for hardened glass heat-treated in-situ at $550 - 630^\circ\text{C}$ (black points) in the regime 70 min at 550°C , temperature increase in 10°C steps and 1 h soaking at each step in the interval $560 - 620^\circ\text{C}$ and finally 30 min at 630°C as well as for samples pre-treated for 18 h from 610 to 670°C (triangles) and samples subjected to isothermal pre-treatment at 670°C for different lengths of time (circles). It is evident that the growth of the sizes of the nonuniformities is accompanied by an increase of the distance between them with prolonged treatment at temperature close to the temperature of the exothermal peak. This attests to a decrease of the interface, i.e., recondensation processes (*Ostwald ripening*) [25], intensifying with increasing temperature and to a lesser extent with increasing heat-treatment time. As a result the fraction of the large phase nano-nonuniformities increases and

Fig. 7. Dependence of heat-treatment conditions for Ge35-0.1 glass on the size of the nonuniformities (a) and a quantity inverse to the scattering vector at the maximum on the low-angle curve q_{\max}^{-1} (b). The dashed line denotes the sizes of the nonuniformities and q_{\max}^{-1} in the initial glass.

the fraction of small ones decreases. This process slows down with increasing distance between the growing nanoparticles and with decrease of their number. Thus, in these glasses near the exothermal peak the nano-nonuniformities stop growing at the size about 20 nm. Such growth stoppage at fixed temperatures had been observed previously in sital-forming glasses in the systems $\text{Li}_2\text{O}-\text{Al}_2\text{O}_3-\text{SiO}_2-\text{TiO}_2$ and $\text{MgO}-\text{Al}_2\text{O}_3-\text{SiO}_2-\text{TiO}_2$ [26, 27].

The presence of broadband luminescence and the comparatively low glassmaking temperature (1480°C) indicate that the nanostructured glasses obtained are promising for the development of fiber amplifiers and broadband sources of radiation in the near-IR range. However, as in the case of Ni^{2+} -doped MgAl_2O_4 single crystal in glass ceramic materials it is possible that induced absorption from a metastable state occurs, which will make it difficult to obtain laser generation.

This work is supported by the RF Ministry of Education and Science (grant 11.G34.310027), the Russian Foundation for Fundamental Research (grant 12-03-317112) and the Kariplo Scientific Research Foundation (grant 2012-0920).

REFERENCES

1. V. N. Sigaev, S. Yu. Stefanovich, B. Champagnon, et al., "Amorphous nanostructuring in potassium niobium silicate glasses by SANS and SHG: a new mechanism for second-order optical non-linearity of glass," *J. Non-Cryst. Solids*, **306**, 238 – 248 (2002).
2. Y. Teng, K. Sharafudeen, Sh. Zhou, and J. Qui, "Glass-ceramics for photonic devices," *J. Ceram. Soc. Jpn.*, **120**, 458 – 466 (2012).
3. G. H. Beall and L. R. Pinckney, "Nanophase glass-ceramics," *J. Am. Ceram. Soc.*, **82**, 5 – 16 (1999).
4. T. Suzuki, K. Horibuchi, and Y. Ohishi, "Structural and optical properties of $\text{ZnO}-\text{Al}_2\text{O}_3-\text{SiO}_2$ system glass-ceramics containing Ni^{2+} -doped nanocrystals," *J. Non-Cryst. Solids*, **351**, 2304 – 2309 (2005).
5. B. Wu, Sh. Zhou, J. Qiu, et al. "Transparent Ni^{2+} -doped $\text{MgO}-\text{Al}_2\text{O}_3-\text{SiO}_2$ glass-ceramics with broadband infrared luminescence," *Chin. Phys. Lett.*, **23**, 2778 (2006).

6. S. Zhou, N. Jiang, H. Dong, et al., "Size-induced crystal field parameter change and tunable infrared luminescence in Ni²⁺-doped high-gallium nanocrystals embedded glass ceramics," *Nanotechnology*, **19**, 015702 (2008).
7. T. Suzuki, G. S. Murugan, and Y. Ohishi, "Optical properties of transparent Li₂O–Ga₂O₃–SiO₂ glass-ceramics embedding Ni-doped nanocrystals," *Appl. Phys. Lett.*, **86**, 131903 – 131906 (2005).
8. T. Suzuki, Y. Arai, and Y. Ohishi, "Crystallization processes of Li₂O–Ga₂O₃–SiO₂–NiO system glasses," *J. Non-Cryst. Solids*, **353**, 36 – 43 (2007).
9. T. Suzuki, Y. Arai, and Y. Ohishi, "Quantum efficiencies of nearinfrared emission from Ni²⁺-doped glass-ceramics," *J. Luminescence*, **128**, 603 – 609 (2008).
10. B. Wu, J. Ruan, J. Ren, et al., "Enhanced broadband near-infrared luminescence in transparent silicate glass ceramics containing Yb³⁺ ions and Ni²⁺-doped LiGa₅O₈ nanocrystals," *Appl. Phys. Lett.*, **92**, 041110 (2008).
11. S. Zhou, G. Feng, B. Wu, et al., "Intense Infrared luminescence in transparent glass-ceramics containing β-Ga₂O₃ : Ni²⁺ nanocrystals," *J. Phys. Chem. C*, **111**, 7335 – 7338 (2007).
12. N. V. Golubev, V. I. Savinkov, E. S. Ignat'eva, et al., "Nickel activated gallium-containing glasses, luminescing in the near-IR range," *Fiz. Khim. Stekla*, **36**, 835 – 842 (2010).
13. V. N. Sigaev, N. V. Golubev, E. S. Ignat'eva, et al., "Nickel-assisted growth and selective doping of spinel-like gallium oxide nanocrystals in germano-silicate glasses for infrared broadband light emission," *Nanotechnology*, **23**, 015708–015715 (2012).
14. V. M. Mashinsky, N. M. Karatun, V. A. Bogatyrev, et al., "Microfluorescence analysis of nanostructuring inhomogeneity in optical fibers with embedded gallium oxide nanocrystals," *Microsc. Microanal.*, **18**, 259 – 265 (2012).
15. V. N. Sigaev, N. V. Golubev, E. S. Ignat'eva, et al., "Native amorphous nanoheterogeneity in gallium germanosilicates as a tool for driving Ga₂O₃ nanocrystal formation in glass for optical devices," *Nanoscale*, **5**, 299 (2013).
16. B. Wu, S. Zhou, J. Ren, et al., "Enhanced luminescence from transparent Ni²⁺-doped MgO–Al₂O₃–SiO₂ glass ceramics by Ga₂O₃ addition," *J. Phys. Chem. Solids*, **69**, 891 – 894 (2008).
17. L. A. Reznitskii, *Calorimetry of Solids (Structural, Magnetic, Electronic Transformations)* [in Russian], Izd. MGU, Moscow (1981).
18. R. Moncorge, J. Thery, and D. Vivien, "Enhancement of fluorescence from octahedrally coordinated Ni²⁺ in LaMgAl₁₁O₁₉ materials by Al³⁺/Ga³⁺ ion substitution," *J. Luminescence*, **43**, 167 – 172 (1989).
19. T. Suzuki, G. S. Murugan, and Y. Ohishi, "Spectroscopic properties of a novel near-infrared tunable laser material Ni: MgGa₂O₄," *J. Luminescence*, **113**, 265 – 270 (2005).
20. T. Wang, Sh. S. Farvid, M. Abulikemu, and P. V. Radovanovic, "Size-tunable phosphorescence in colloidal metastable γ-Ga₂O₃ nanocrystals," *J. Am. Chem. Soc.*, **132**, 9250 – 9252 (2010).
21. S. K. Dubrovo and I. S. Lileev, "Glassy gallosilicates and their properties," *Zh. Prikl. Khim.*, **33**, 1471 – 1476 (1960).
22. J. H. Campbell, T. I. Suratwala, C. B. Thorsness, et al., "Continuous melting of phosphate laser glasses," *J. Non-Cryst. Solids*, **263 – 264**, 342 – 357 (2000).
23. M. K. Murphy and K. Emery, "Properties and structure of glasses in the system M₂O–Ga₂O₃–GeO₂ (M = Li, Na, K)," *Phys. Chem. Glasses*, **8**, 26 – 29 (1967).
24. K. Tanaka, T. Mukai, Ts. Ishiham, et al., "Preparation and optical properties of transparent glass-ceramics containing cobalt (II) ions," *J. Am. Ceram. Soc.*, **76**, 2839 – 2845 (1993).
25. N. S. Andreev, O. V. Mazurin, E. A. Porai-Koshits, et al., *Liquation Phenomena in Glasses* [in Russian], Nauka, Leningrad (1974).
26. V. V. Golubkov, O. S. Dymshits, and A. A. Zhilin, "Effect of nickel oxide addition on phase decomposition in lithium-aluminum-silicate glasses containing titanium dioxide," *Fiz. Khim. Stekla*, **10**, 155 – 161 (1984).
27. V. V. Golubkov, O. S. Dymshits, and A. A. Zhilin, "On phase separation and crystallization of glasses in the system MgO–Al₂O₃–SiO₂–TiO₂," *Fiz. Khim. Stekla*, **29**, 359 – 377 (2003).
28. N. V. Kuleshova, V. G. Shcherbitsky, V. P. Mikhailov, et al., "Spectroscopy and excited-state absorption of Ni²⁺-doped MgAl₂O₄," *J. Luminescence*, **71**, 265 – 268 (1997).